Science Advances
AAAS

advances.sciencemag.org/cgi/content/full/5/5/eaav3430/DC1

Supplementary Materials for

Dynamically controllable polarity modulation of $MoTe_2$ field-effect transistors through ultraviolet light and electrostatic activation

Enxiu Wu, Yuan Xie, Jing Zhang, Hao Zhang, Xiaodong Hu, Jing Liu*, Chongwu Zhou*, Daihua Zhang*

*Corresponding author. Email: jingliu_1112@tju.edu.cn (J.L.); chongwuz@usc.edu (C.Z.); zhangdaihua@gmail.com (D.Z.)

Published 3 May 2019, *Sci. Adv.* **5**, eaav3430 (2019)
DOI: 10.1126/sciadv.aav3430

This PDF file includes:

Supplementary Materials and Methods

S1. Atomic force microscopy (AFM) characterization of the device

AFM measurements indicate that the thicknesses of $MoTe_2$ and h-BN are around 28 nm and 11.5 nm, respectively, as shown in fig. S1.

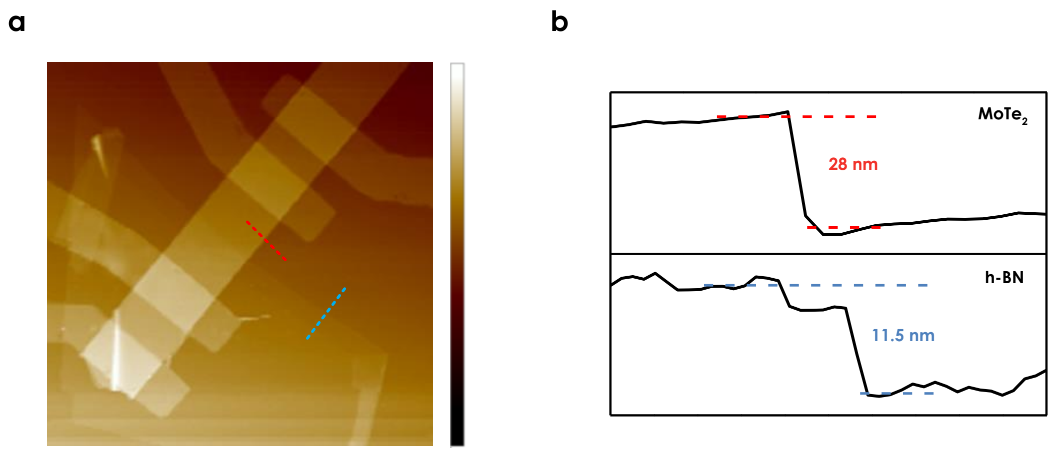

Fig. S1. AFM images of devices. (**a**) AFM image of the whole device. (**b**) Height images of the different regions as highlighted on the device.

S2. Output characteristic curves of Device A and B at different V_{gs} under different light illumination

Notably, as shown in fig. S2d, output characteristics of Device B at different V_{gs} under UV illumination exhibited almost negligible gate modulation with source-drain current of pA level, which is consistent with transfer characteristic as shown in Fig. 1e.

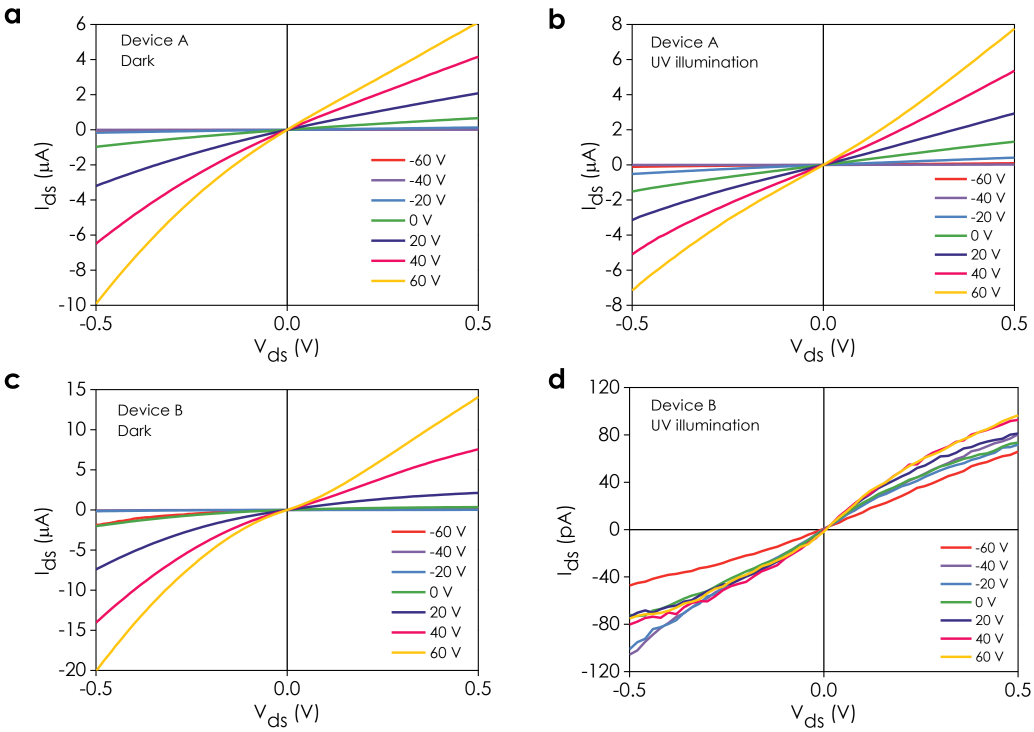

Fig. S2. Output characteristic curves of device A and device B. Output characteristics of Device A in dark (**a**) and UV illumination (**b**), respectively. Output characteristics of Device B in dark (**c**) and UV illumination (**d**) respectively.

S3. Position of minimum conduction point (MCP) versus writing voltage in p-type and n-type doping processes

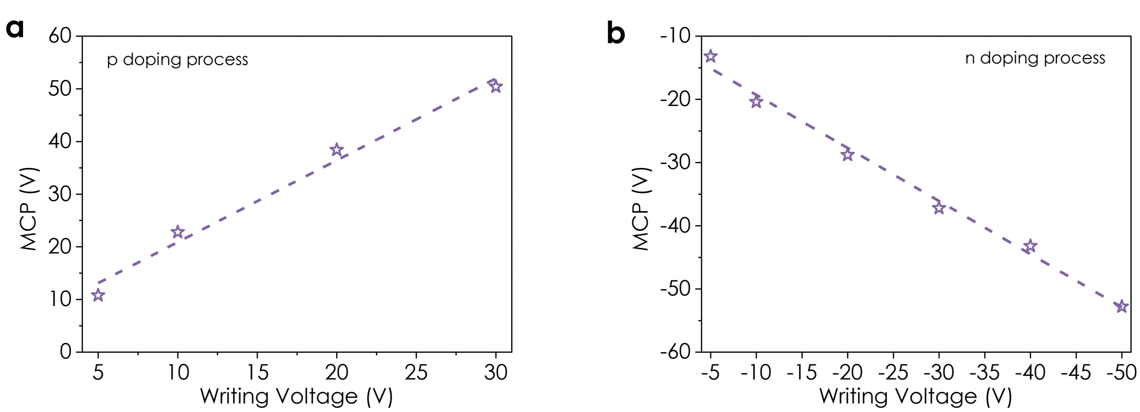

Fig. S3. Position of MCP versus writing voltage in the p-type and n-type doping processes. Position of minimum conduction point in p-type doping (**a**) and n-type doping (**b**) processes extracted from transfer characteristic curves in Fig. 2a and c. Data points for writing voltages of $V_{gs} > +30$ V and $V_{gs} < -60$V are missing as the device became completely unipolar in these regions.

S4. Transport properties of photo-doped $MoTe_2$/BN devices with different thicknesses of $MoTe_2$ and BN

As shown in fig. S4, the thickness of BN ranges from 5.6 to 24 nm, while the thickness of $MoTe_2$ ranges from 4.0 to 28 nm. Consistently with the text, the original devices exhibited ambipolar transport property. We exposed the devices to UV illumination for 1 second at writing voltage = 60 V (writing voltage = -60 V) to achieve p-type doping (n-type doping) of devices, which indicates excellent reproducibility of this doping process.

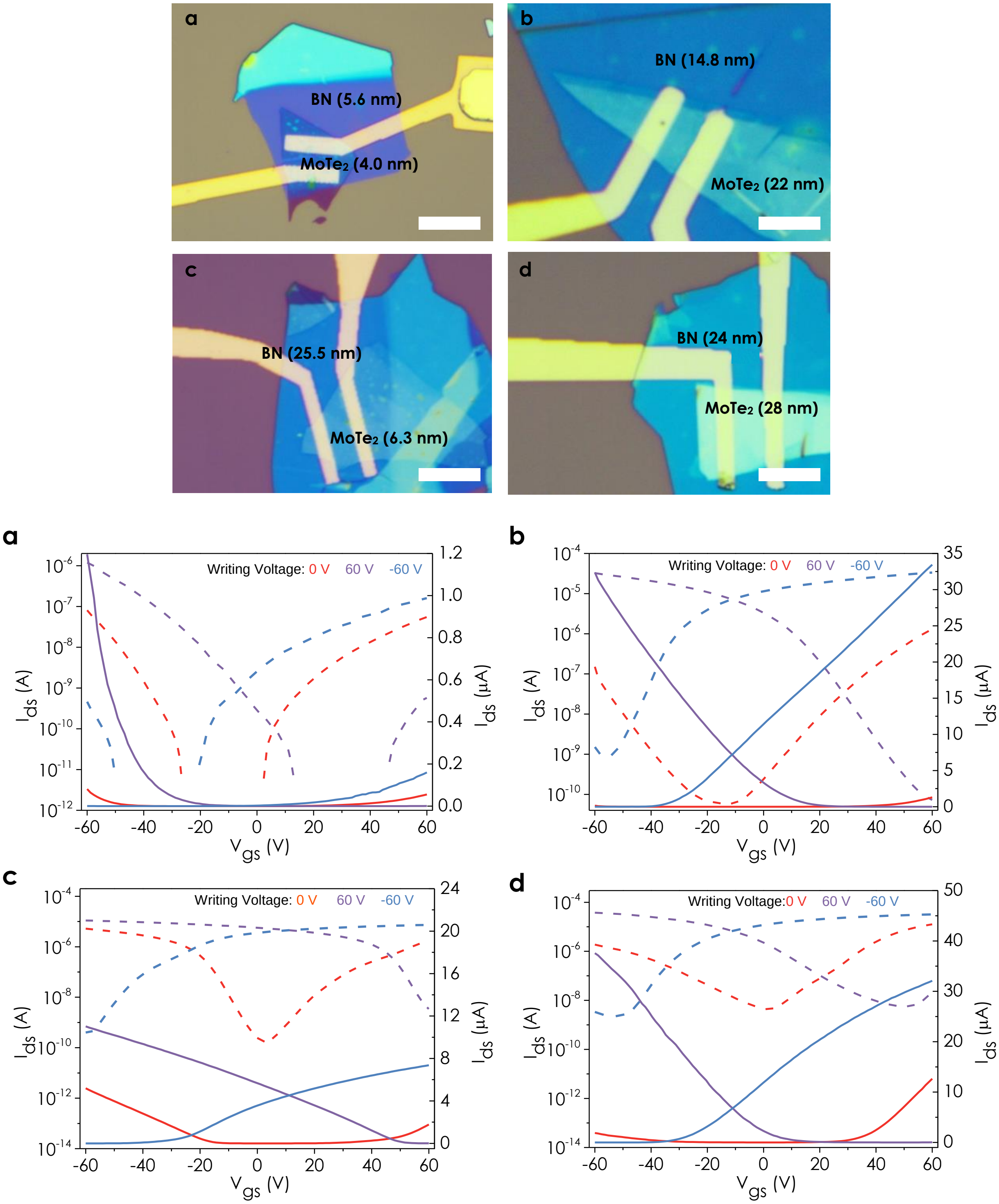

Fig. S4. Transfer characteristics of four other $MoTe_2$ samples under different doping conditions. (**a**), (**b**), (**c**), (**d**) Optical microscopy images and corresponding transfer characteristics of four other sample devices under different doping condition.

S5. Transport properties of photo-doped WSe_2/BN and MoS_2/BN heterostructure

The WSe_2-based transistors exhibit ambipolar transfer characteristic as shown in red curves of fig. S5b. The WSe_2/h-BN device exhibits significant p-type and n-type enhancement after being exposed to UV illumination for 1 second at writing voltage = 0 V, 60 V, -60 V, respectively. Due to the strong pinning effect at metal-MoS_2 interface, the p-type MoS_2 transistors are seldomly achieved. We also face the same predicament using this doping technology, as shown in fig. S5d. After exposing MoS_2/BN device in UV illumination for 1 second at writing voltage = 60 V, the p-regime of MoS_2 shows negligible enhancement, but the current of n-regime of MoS_2 decrease evidently.

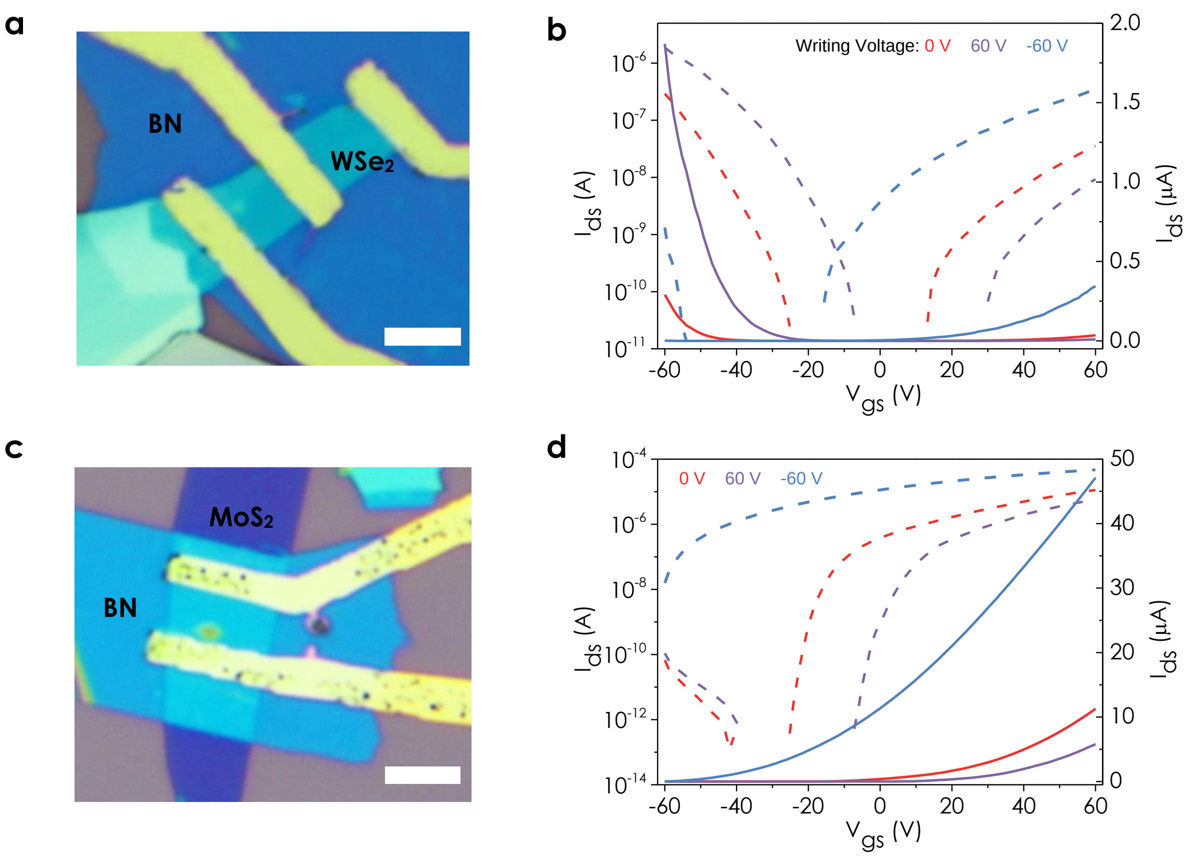

Fig. S5. Transfer characteristics of WSe_2 and MoS_2 under different doping conditions. Optical microscopy images of fabricated WSe_2/h-BN (**a**) and MoS_2/h-BN (**c**) devices. Scale bar is 5 um. Transport characteristics of WSe_2/h-BN (**b**) and MoS_2/h-BN (**d**) after photoinduced modulation doping.

S6. Transport properties of $MoTe_2$ on bare SiO_2 substrate under different various doping conditions

As shown in fig. S6, the red trace is the transfer characteristic of $MoTe_2$ device in the darkness. The violet and blue traces are transfer characteristics of $MoTe_2$ device after being exposed to UV light for 1 seconds at writing voltage = 0 V, -60 V and 60 V, respectively. We found that there was no p/n-doping effect in device, which indicates that the h-BN plays an important role in the UV-induced doping process.

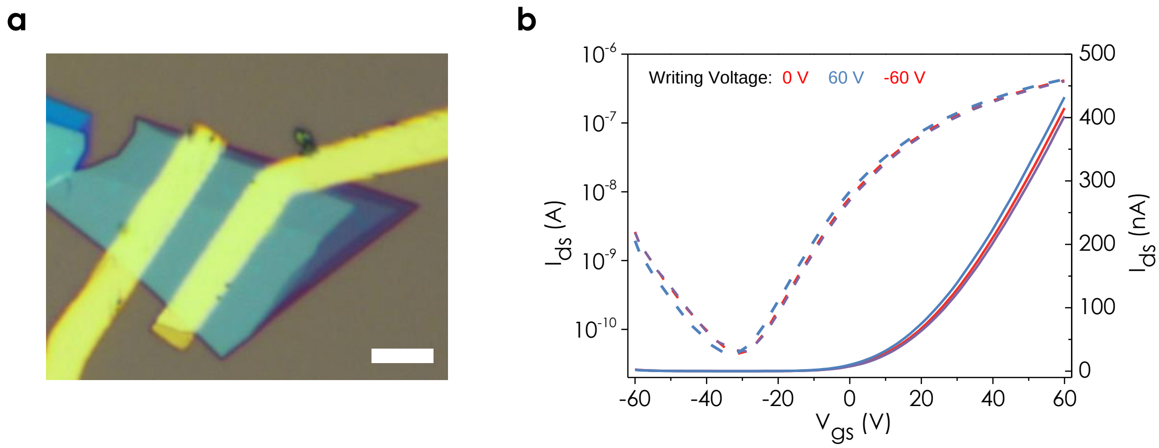

Fig. S6. Transfer characteristics of $MoTe_2$ on SiO_2 substrate under different conditions. (**a**) Optical microscopy image of $MoTe_2$ transistor on SiO_2 substrate. (**b**) Transport properties of $MoTe_2$ on bare SiO_2 substrate under different doping conditions.

S7. Doping behaviors of the $MoTe_2$/BN device under visible light illumination

We explore the doping behaviors of $MoTe_2$/BN device under visible light illumination for 5 min at writing voltage = 0 V, -60 V and 60 V, respectively. The wavelengths of visible light are 400 nm and 500 nm, respectively.

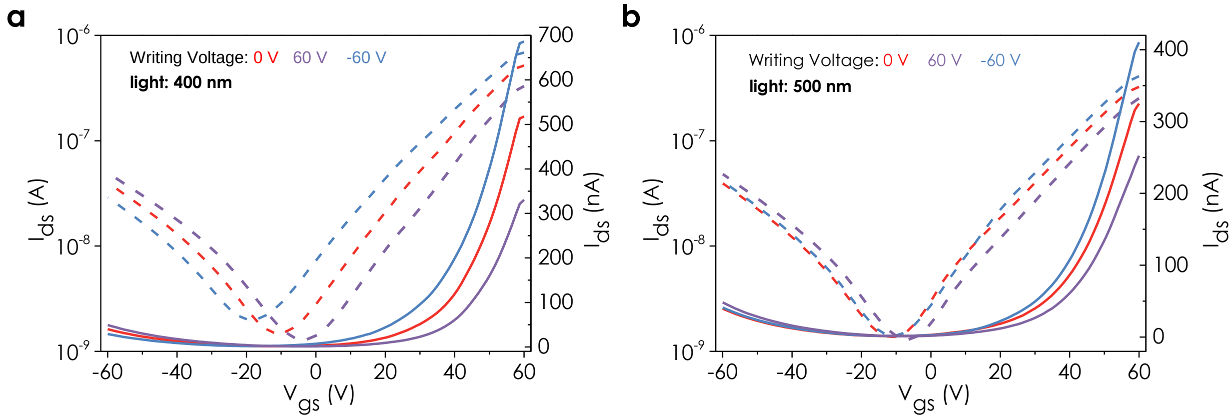

Fig. S7. Doping behaviors of the $MoTe_2$/BN device under visible light illumination. Transfer characteristics of $MoTe_2$/BN device after being exposed to visible light illumination at wavelength of 400 nm (**a**) and 500 nm (**b**), respectively.

S8. Dynamic photo-response of the device at different V_{ds}

Figure S8 shows dynamic photo-response of the device. The power of incident light is 1.25 nW. At V_{ds} = 0 V, the response time of device is ~ 2 ms. The device exhibited positive photoresponse and showed a maximum photo-detection responsivity of 31.4 A/W at V_{ds} = 1 V. Moreover, the response time is shorter than 200 us, significantly enhanced by one order of magnitude compared with the response at V_{ds} = 0 V.

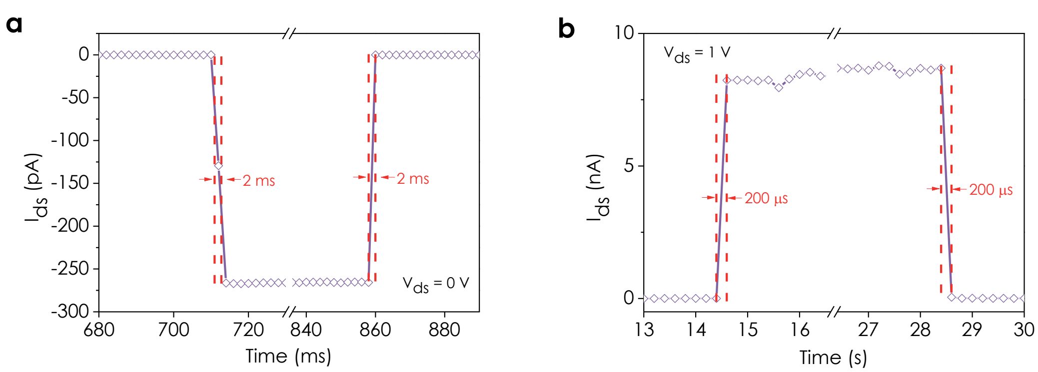

Fig. S8. Dynamic response characteristics of device C at different V_{ds}. Dynamic photo-response of the device at V_{ds} = 0 V (**a**) and V_{ds} = 1 V (**b**), respectively.